-

Inversion, Assessment of Stability and Uncertainty of Geoelectric Sounding data using a New Hybrid Meta-heuristic algorithm and Posterior Probability Density Function Approach

Kuldeep Sarkar, Upendra K. Singh*

Department of Applied Geophysics, IIT (ISM), Dhanbad 826004, Jharkhand, India

*Correspondence: upendra@iitism.ac.in

ABSTRACT

Estimating a reliable subsurface resistivity structure using conventional techniques is challenging due to the nonlinear nature of the inverse problems. The performance of the inversion techniques can be pretty ambiguous based on the optimal error. Although traditional methods have proven to be quite effective. The impact of the constraints accessible from the borehole is examined for further assessment and enhance the algorithm's effectiveness. The vPSOGWO is a new approach based on model search space without any prior information. This new strategy describes the hybridization of the particle swarm optimizer (PSO) with the grey wolf optimizer (GWO). To understand the efficiency and novelty of the algorithm, it has been validated on two different kinds of synthetic resistivity data with various sets of noise and finally applied on three field datasets of different geological terrains. The analyzed results suggest that the subsurface resistivity model shows considerable uncertainty. Thus, it is superior to examine the histograms and posterior probability density functions (PDF) of such solutions for exemplifying the global solution. PDF with 68.27% CI selects a region with a higher probability. Therefore, the inverted models are used to estimate the mean global solution and the most negligible uncertainties, where the mean global solution represents the best solution. Our vPSOGWO inverted outcomes have been proven to be more accurate than classic PSO, GWO and state-of-art

-

variant of classic approaches. As a results, this novel method plays a vital role in DC data inversion effectively.

Keywords**:** vPSOGWO, Uncertainty, Stability, Inversion, Resistivity data.

1. INTRODUCTION

The vertical electrical resistivity sounding (VES) method is an economical and simple method due to a wide application such as hydrogeological, groundwater, minerals, geothermal, hydrocarbon, engineering, environmental fields, etc. (Sen et al., 1993, Sharma, 2012, Panda et al., 2018), which have been used for determining the layered parameters. The VES data interpretation is challenging due to its unstable, nonunique solution and algorithm sensitivity (Narayan et al., 1994, Oldenburg and Li, 1994, Singh et al., 2005, 2013). Therefore, many researchers have developed several inversion algorithms to improve the accuracy, stability and reduce the uncertainty of the solutions. These inversion techniques are grouped into local and global optimization techniques. In the local inversion techniques, a logical initial guess is required to get the solution. The researchers have led to think about alternative methods, where a broad range of parameters can be established. Many researchers have developed various metaheuristic optimization algorithms to solve various real-world problems. These algorithms inspired from the natural phenomenon include Ant Colony (Colorni et al., 1991), Bat algorithm (Yang, 2010), Biogeographically based Optimization (Simon, 2008), Differential Evolution (Storn and Price, 1997), Firefly algorithm (Yang, 2010), Genetic Algorithm (Whitley, 1994; Mitchell, 1996), Gravitational Search Algorithm (Rashedi et al., 2009), Grey Wolves Optimizer (Mirjalili et al., 2014), Particle Swarm Optimization (Kennedy and Eberhart, 1995), etc. These optimization techniques aim to have an optimum solution and fast convergent rate to obtain global minima. However, unique characteristics, viz. exploration and exploitation, in global optimization algorithms persist.

For example, the Particle Swarm Optimization (PSO) algorithm has very high potential in exploitation, implies that the algorithm performs well in local search (Senel et al., 2019) but is inferior in exploration, which means the algorithm has less ability to find out the starting position near-global minima and because of low exploration characteristics, it gets trapped at the local minima (Eiben and Schippers, 1998, Mirjalili and Hashim, 2010). So, integrating the two algorithms with opposite characteristics is the best way to solve the exploration characteristics and exploitation characteristics, and provide more accurate and reliable solution than results obtained from an individual's algorithm. Many authors have developed various hybrid metaheuristic algorithms such as PSOGA for fundamental function analysis, PSOACO for data mining, PSODE for global optimization using the standard function, and PSOGSA using the standard function (Esmin et al., 2013; Lai and Mingyi, 2009; Rashedi et al., 2009).

This study focuses on a variable weight hybrid algorithm that fuses the exploration ability of Particle Swarm Optimizer (PSO) with the exploration ability of Grey Wolves Optimizer (GWO), known as vPSOGWO (Şenel et al., 2019). In this algorithm, some random particles of PSO are replaced by the new ones obtained from GWO. Earlier the constant weight hybrid technique of PSO and GWO known as HPSOGWO has been used in different applications by some authors, such as for single area unit commitment problems (Kamboj, 2015), mathematical problems (Singh and Singh, 2017), and benchmark functions and real-world issues (Senel et al., 2019). But none of the researchers have tested the current work in geophysical data inversion to the best of our information. Thus, the applicability of the vPSOGWO algorithm is demonstrated on synthetic data with noise, without noise, and various field resistivity sounding data for estimating the resistivity distribution in a 1D earth's subsurface model. The study also calculate the posterior probability density functions (PDF) with 68.27% confidence interval and

-

correlation matrix on all accepted models for determining mean global model and uncertainty. As a result, we analysed and compared the effectiveness of the proposed algorithms with classical PSO, GWO and state-of-art variant of classic methods. Our analysis advocates that the vPSOGWO algorithm produces a more accurate and reliable model with excellent stabilities and the least uncertainty in the model independently, as well as the ability to successfully resist noise.

2. FORWARD MODELLING ALGORITHM

The forward code is developed, and synthetic resistivity data sets were created using the kernel function (Koefoed, 1979) with Schlumberger resistivity configuration (*Fig. 1*) from known parameters such as current electrode spacing, number of geological multilayers of true resistivity their thickness. The mathematical expression for apparent resistivity is given as:

$$\boldsymbol{\rho_a}(\boldsymbol{s},\boldsymbol{m}) = \rho_1 + \boldsymbol{s}^2\rho_1 \int_0^\infty T_1(\boldsymbol{\lambda},\boldsymbol{m})\ \boldsymbol{J_1}(\boldsymbol{\lambda s})d\lambda \tag{1}$$

where, $\boldsymbol{J_1}$ is the first order Bessel function, $\boldsymbol{\lambda}$ is the integration variables, $\boldsymbol{s}$ is half of the current electrode spacing, $\boldsymbol{m}$ is the model. $\boldsymbol{T_n}$ is the kernel's resistivity transform, $\boldsymbol{\rho_k}$ is the resistivity and $\boldsymbol{t_k}$ is the thickness of the kth layers.

For each layer, the kernel's resistivity transform T_k has been determined by Pekeris (1940). The apparent resistivity, $\boldsymbol{T_k(\lambda)}$, is convolution with linear filter theory to compute as:

$$\boldsymbol{T_k}(\boldsymbol{\lambda}) = \boldsymbol{\rho_k} * (\boldsymbol{T_{k+1}}(\boldsymbol{\lambda}) + \boldsymbol{\rho_k} \tanh(\lambda \boldsymbol{t_k}))/(\boldsymbol{\rho_k} + \boldsymbol{T_{k+1}}(\boldsymbol{\lambda}) \tanh(\boldsymbol{\lambda t_k})) \tag{2}$$

-

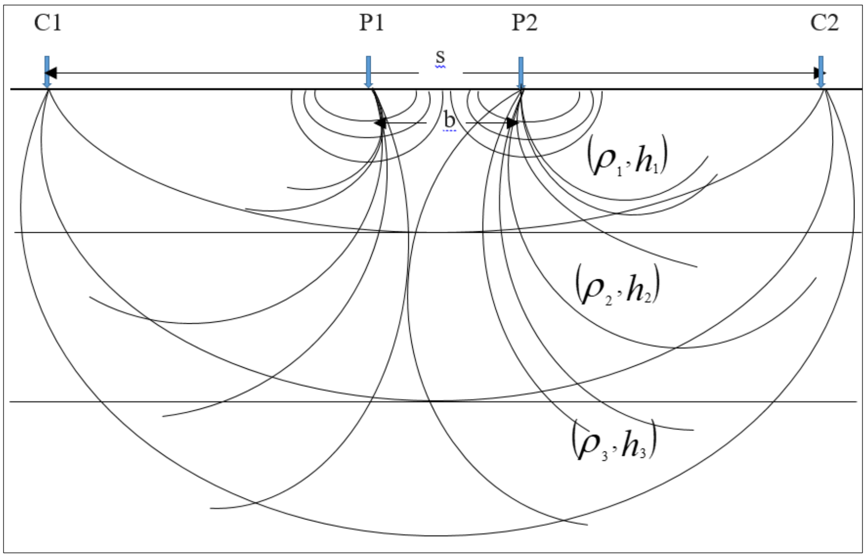

Figure 1. Schlumberger array configuration for three layer case, where C1 and C2, through which current is injected, are current electrode with spacing s; P1 and P2 are potential electrodes with spacing b.

3. INVERSE MODELLING ALGORITHM

The geophysical inverse problem can be formulated through forward modelling operator/functional to aim at achieving the geophysical model/solution, which illuminates the observed data in the best. This operator integrates the geophysical problems and maps between the observed data ***y*** and the solution ***x*** as:

$$\boldsymbol{y} = f(\boldsymbol{x}) \qquad (3)$$

Inversion set up finding a model that minimizes cost function/misfit functional that generally is a degree of the relationship between the N number of observed data (y_o) and the calculated data (y_c). This misfit functional can be introduced here as a mean-square-error (MSE) and can be defined as:

$$\text{MSE} = \frac{1}{N}\sum_{i=1}^{N}(y_o - y_c)^2 \qquad (4)$$

-

3.1. Particle swarm optimization

Particle swarm optimization (PSO) is based on the social behavior of animals such as schooling of fish or flocking of bird (Kennedy and Eberhart in 1995). When the birds go in search of food, they scattered randomly within the search space before they can determine the position of food. While searching for food, there is always a bird who is aware of the position of food. This information they share with others. In this method, each bird is called as particle which is represented by geophysical solutions/models (i.e., here particle is resistivity layer parameters). The capability/fitness of each swarm/birds is estimated between the N number of observed data (y_o), which measure the swarm and the food distance, and the computed data ($\boldsymbol{y}_c$) which measures the swarm and the estimated position (resistivity layer parameter/solution) of the prey distance using equation 4.

The best position among particles with information about it are store for each iteration in memory. The new velocity and position of the population pool are accepted if its possibility is large, otherwise it is rejected. In that case, the particles are randomly distributed in the search space in order to escape the local optima. The search continues until it gains maximum possibility or it reaches the maximum iteration. In global search space, the position of each particle is updated by the following two mathematical equations:

$$\vec{\boldsymbol{v}}_i(t+1) = \vec{\boldsymbol{v}}_i(t) + c_1 \times rand\left(\vec{\boldsymbol{x}}_p(t) - \vec{\boldsymbol{x}}_i(t)\right) + c_2 \times rand \times \left(\vec{\boldsymbol{x}}_g - \vec{\boldsymbol{x}}_i(t)\right) \quad (5)$$

$$\vec{\boldsymbol{x}}_i(t+1) = \vec{\boldsymbol{x}}_i(t) + \vec{\boldsymbol{v}}_i(t+1) \quad (6)$$

Here, $\vec{\boldsymbol{v}}_i$ represent the velocity of the i^{th} particle with position $\vec{\boldsymbol{x}}_i$, $\vec{\boldsymbol{x}}_p$ is the best position obtained by the i^{th} particle, $\vec{\boldsymbol{x}}_g$ is the best position, t is the number of the iteration, i represents the number of the model ($i = 1, 2, 3, \ldots, N$), $rand$ represent the random values with range [0,1], and the coefficient $c_1$and c_2 represent the optimization parameter. The

-

disadvantage of PSO algorithm is that, while directing particles to random positions, it has small possibility to escape the local minima.

3.2 Grey wolf optimization

Grey wolf optimization (GWO) algorithm mimics the leadership hierarchy and hunting mechanics of grey wolves, and used its ability to solve the standard and real-life problems. In the grey wolf's community, they are divided in four groups: (i) the alpha, (ii) the beta, (iii) the delta and (iv) the omega, in which alpha, beta and delta are the fittest wolves, who guide omega towards promising areas of the search space. The alpha is the leader, which generally makes important and final decision for all the wolves so and represents the fittest solution. The betas are subordinates that help the alphas in their decision making but they cannot force them in any decision. They can only order the lower wolves. The beta group takes the order from alpha group which they reinforce throughout the other group and send back the feedback to the alpha. All the groups dominate over the omega wolves. The omega group is an important part during hunting as they play role of the scapegoat and are always allowed to eat at the end. If a wolf is not the part of alpha, beta or omega group, then they are known as delta which only summit to alpha and beta groups. In GWO algorithm, the alpha group represents the best position, i.e., geophysical model/solution. In our case geophysical model is resistivity layer parameters. The beta and delta groups are consecutive best solutions and omega group is the best solution that follows always the other groups. The capability/fitness of each wolf is estimated between the observed data (which measures wolf and prey distance) and the computed data (which measures the wolf and the estimated position of the prey distance) using equation 4.

Hunting in the grey wolf's community has been divided into three groups: prey search, encircling the prey, and attacking the prey. The encircling nature of the wolves is defined by the following equation:

$$d = |c \times (t) - \vec{\boldsymbol{x}}_i(t)| \tag{7}$$

$$\vec{\boldsymbol{x}}_i(t+1) = \vec{\boldsymbol{x}}_p(t) - a \times d \tag{8}$$

where, $\vec{\boldsymbol{x}}_p$ is the prey position, $\vec{\boldsymbol{x}}_i$ is the grey wolf's positions, a and c are the vectors mathematically formulated as:

$$a = a_1 \times (2 \times rand - 1) \tag{9}$$

$$c = 2 \times rand \tag{10}$$

Here, $a_1 = 2 \times (1 - t/l)$ which varies from 2 to 0 in decreasing order with increasing iteration *(t)*, l represent the maximum iteration, and rand is the random number between [0,1].

The alpha group led the grey wolves' community, in which the beta and the delta group to search the prey location and the omega groups follow them. The alpha group wolves gives the best solution, while the second and third best solution is provided by the beta and the delta group wolves, respectively. Therefore, the rest community wolves i.e., omega group wolves follows the best solution wolves to obtain best location. This is mathematical equated by:

$$d_{\alpha,\beta,\delta} = |\vec{\boldsymbol{c}}_{1,2,3} \times \vec{\boldsymbol{x}}_{\alpha,\beta,\delta} - \vec{\boldsymbol{x}}| \tag{11}$$

The best location/position for alpha, beta and delta wolves in each iteration is given by $\vec{\boldsymbol{x}}_\alpha$, $\vec{\boldsymbol{x}}_\beta$ and $\vec{\boldsymbol{x}}_\delta$, respectively.

$$\vec{\boldsymbol{x}}_{1,2,3} = |\vec{\boldsymbol{x}}_{\alpha,\beta,\delta} - \vec{\boldsymbol{a}}_{1,2,3} \times \vec{\boldsymbol{d}}_{\alpha,\beta,\delta}| \tag{12}$$

Here, $\vec{\boldsymbol{x}}_p(t+1)$ describe the updated position of the prey in $(t+1)$ iteration which is obtained from the mean position of three best wolves in the population, that is,

$$\vec{\boldsymbol{x}}_p(t+1) = (\vec{\boldsymbol{x}}_1 + \vec{\boldsymbol{x}}_2 + \vec{\boldsymbol{x}}_3)/3 \tag{13}$$

The values of a are utilized by wolves which force the search to move away from the prey. When $a \geq 1$, the hunting is abandoned in order to have a better solution and, when $a < 1$, the wolves are enforced to attack the prey. In equation 9, a varies between $[-2a_{1,}\ \ 2a_1]$.

3.3 Hybrid variable weighted PSOGWO (vPSOGWO)

Despite its usefulness in achieving successful results in real-world problems, it tends to fall into the local minima, causing the solution to move away from global minima. This tendency for deteriorating within the local minima is stopped by the exploration ability of the GWO algorithm. Therefore, the hybrid variable weighted PSOGWO, known as vPSOGWO that fuses the exploitation potential of PSO with the exploration potential of GWO to overcome each other's discrepancy with the implementation of varying weight. Due to the involvement of two distinct variants running together to solve the problem, this hybrid vPSOGWO is called a co-evolutionary hybrid algorithm. The encircling behaviour of each wolf is updated by the following equations:

$$\vec{\boldsymbol{d}}_{\alpha,\beta,\delta} = |\vec{\boldsymbol{c}}_{1,2,3} \times \vec{\boldsymbol{x}}_{\alpha,\beta,\delta} - w \times \vec{\boldsymbol{x}}| \quad (14)$$

Here, $w = w_{max} - (w_{max} - w_{min}) \times t/l$ (15)

Here, $w_{max} = 0.9$, and $w_{min} = 0.2$ are found more appropriate after tuning for our study.

The best location/position (geophysical model) for alpha, beta and delta wolves in each iteration is given by $\vec{x}_\alpha$, $\vec{x}_\beta$ and $\vec{x}_\delta$, respectively.

$$\vec{\boldsymbol{x}}_{1,2,3} = |\vec{\boldsymbol{x}}_{\alpha,\beta,\delta} - \vec{\boldsymbol{a}}_{1,2,3} \times \vec{\boldsymbol{d}}_{\alpha,\beta,\delta}| \quad (16)$$

where,

$$a_{1,2,3} = a_1 * (2 * rand - 1) \quad (17)$$

$c_{1,2,3} = 0.5$ (chosen after tuning) (18)

$$a_1 = 2 * (1 - t/l) \tag{19}$$

The updated velocity and position of vPSOGWO are:

$$\vec{\boldsymbol{v}}_i(t+1) = w \times \vec{\boldsymbol{v}}_i(t) + c_1 \times rand \times \left(\vec{\boldsymbol{x}}_1 - \vec{\boldsymbol{x}}_i(t)\right) + c_2 \times rand \times \left(\vec{\boldsymbol{x}}_2 - \vec{\boldsymbol{x}}_i(t)\right) + c_3 \times rand \times (\vec{\boldsymbol{x}}_3 - \vec{\boldsymbol{x}}_i(t)) \tag{20}$$

$$\vec{\boldsymbol{x}}_i(t+1) = \vec{\boldsymbol{x}}_i(t) + \vec{\boldsymbol{v}}_i(t+1) \tag{21}$$

Here, the value 1.5 for each coefficients c_1, c_2, and c_3 after tuning the parameters found more suitable in the present study (Roshan and Singh, 2017).

---

vPSOGWO algorithm

Max_Iter: maximum iterations set

Pop_no: population size

Para: Number of parameters

Fitness=infinite: already set

Lb and *Ub*: set Lower bound (*Lb*) and Upper bound (*Ub*) for different parameters

Initialize particles randomly

Procedure

for *l* = 1 to *Max_Iter* do

    for *i* = 1 to *Pop_no* do

        for *j* = 1 to *Para* do

            check the *Lb* and *Ub* for randomly created particles

        end

    end

    for *i* = 1 to *Pop_no* do

-

Calculate the *fitness* form cost function

Update the wolves' fitness and position

end

Update *a1*, *a*, *c*, *w*, using equations (15-17), (13)

for i = 1 to *Pop_no* do

for j = 1 to *Para* do

Update position of $\vec{\boldsymbol{x}}_1$, $\vec{\boldsymbol{x}}_2$ and $\vec{\boldsymbol{x}}_3$ using equations (14) and (16)

Update best particle velocity and position using equations (20-21)

end

end

end

4.0 Statistical simulation for global model and uncertainty estimation

The proposed algorithms yield good-fitting models, but the evaluation of a global solution requires numerous techniques. It is noteworthy for selecting the region of solution/model search space, where we find enormous solutions. The methods for selecting the region of model space were selected to envisage the global solution and reduce the uncertainty in the ultimate solution (Mosegaard and Tarantola, 1995; Sen and Stoffa, 1996). Thus, many solutions and associated error estimated were kept in memory for consequent statistical measurements. Therefore, 10^8 solutions were generated for each algorithm using logarithmic mean square error, and every computed response corresponding to each model fits well with the observed response. However, the model parameters obtained may differ from each other, which lie within the search range in multidimensional space. Hence, the mean model from the model parameters is defined as (Ross, 2009):

$$\widehat{\boldsymbol{m}}_i = \frac{1}{M}\sum_{j=1}^{M}\boldsymbol{m}_{i,j} \tag{20}$$

-

where i =1 to the total number of the parameters, M is the total models and $\boldsymbol{m}_{i,j}$.

All algorithms are executed for 10,000 runs with 1000 iterations to obtain the best model parameters. It is noteworthy to mention that in vPSOGWO, multiple runs are crucial because 1000 weightage points are laying in between the inertial weights of 0.9 to 0.2, such that each weightage point yields a fitted model in a run. As a result, 10,000 runs provide 10,000 chances to each weightage point to fetch the best-fitted model.

Therefore, the posterior covariance matrices are defined in the equation (Ross, 2009):

$$Cov(\boldsymbol{m}_{i,k}) = \frac{1}{M-1}\sum_{j=1}^{M}\left(\boldsymbol{m}_{i,j} - \widehat{\boldsymbol{m}}_i\right) \times \left(\boldsymbol{m}_{k,j} - \widehat{\boldsymbol{m}}_k\right) \tag{21}$$

and posterior correlation matrices are described in the equation:

$$Corr(\boldsymbol{m}_{i,k}) = Cov(\boldsymbol{m}_{i,k})/\sqrt{Cov(\boldsymbol{m}_{i,i}) \times Cov(\boldsymbol{m}_{k,k})} \tag{22}$$

where i and k lie between 1 to total number of parameters.

The square-rooted diagonal elements of the covariance matrix define the uncertainty of the solution, and the correlation matrix gives a rough idea about the relation between the model parameters. If the parameters don't provide a global solution, then the apparent resistivity curve corresponding to the mean model will not adequate the observed value. The posterior correlation matrix corresponding to the indigenous solution will not yield an actual correlation between the parameters obtained via linear regression. For further analysis, posterior PDF and histogram are calculated over all accepted models. The one-dimensional posterior probability density function for various parameters with mean $\widehat{m}_i$ and standard deviation σ_i is given as (Ross, 2009):

$$p(\boldsymbol{y_i}, \widehat{\boldsymbol{m}}_i, \boldsymbol{\sigma_i}) = \left(1/\boldsymbol{\sigma_i}\sqrt{2\pi}\right) \times \exp(-(\boldsymbol{y_i} - \widehat{\boldsymbol{m}}_i)^2/2\boldsymbol{\sigma_i}^2) \tag{23}$$

where y is the solution/model parameter's output store after 10,000 runs of an algorithm and i = 1 to the number of model parameters.

-

Different techniques are based on the posterior PDF to obtain the global solution. One of the techniques is to pick the model parameters with the highest probability values. Another method based on PDF is to normalize (0 to 1) each model parameter by their respective highest probability values. The best model is considered to have the highest sum of normalized probability values (Sharma, 2012). Further, the best model can also be determined by taking the mean of each parameter with probably more significance than the threshold probability. However, these techniques fail to provide the global model.

Therefore, proceeding with a new approach to the study by introducing a confidence interval (CI) more significant than 68.27% as a benchmark for all model parameters. According to the empirical rule, 68.27% of the data lies within the one standard deviation of the mean (Ross, 2009). Thus, the model parameters below 68.27% CI are discarded, and the remaining parameters are used for determining the mean solution and uncertainty. It means that the model represents the global solution with less uncertainty.

5.0 Computation information

The code was developed in MATLAB R2019a in Windows 10 platform having configuration: Model-HP Z240 Tower Workstation, Processor- Intel Xeon CPU E3-1225 v6 @ 3.30GHz, 32.0 GB RAM, 64-bit operating system (OS). However, Global optimization is a time-consuming process, as it requires many forwarding calculations to obtain the best-fitted result.

6.0 Results and discussion

The applicability of the new algorithm vPSOGWO, GWO, and PSO has been assessed inverting several cases of synthetic and field data extracted from different geological terrains (Dixon & Doherty, 1977; Panda et al., 2017). Both synthetic and field data sets were computed and optimized using the developed algorithms, keeping the ten population size and 1000 iterations for 10,000 runs, leading each algorithm to analyzed 10^8 models. We have discussed the inverted results of algorithms to the application on few examples of synthetic and field cases:

6.1 Example 1: Synthetic data- Three-layer case

Initially, to access the applicability and efficacy of the proposed algorithms, a synthetic apparent resistivity sounding data measured with Schlumberger array is generated considering the three-layered earth model sandwich with a high resistive layer of 500.0Ωm and thickness 150.0 m between two low resistive layers of 8.0Ωm and 5.0Ωm. The synthetic data is computed in the Matlab environment as shown in *Fig. 2(a)* with the (*) mark. *Fig. 2* shows (a) the three-layer synthetic data with the best fitted calculated apparent resistivity curve (> 68.27% PDF) and (b) one-dimensional mean model (> 68.27% PDF) for true model (black color), vPSOGWO (red color), GWO (blue color) and PSO (green color).

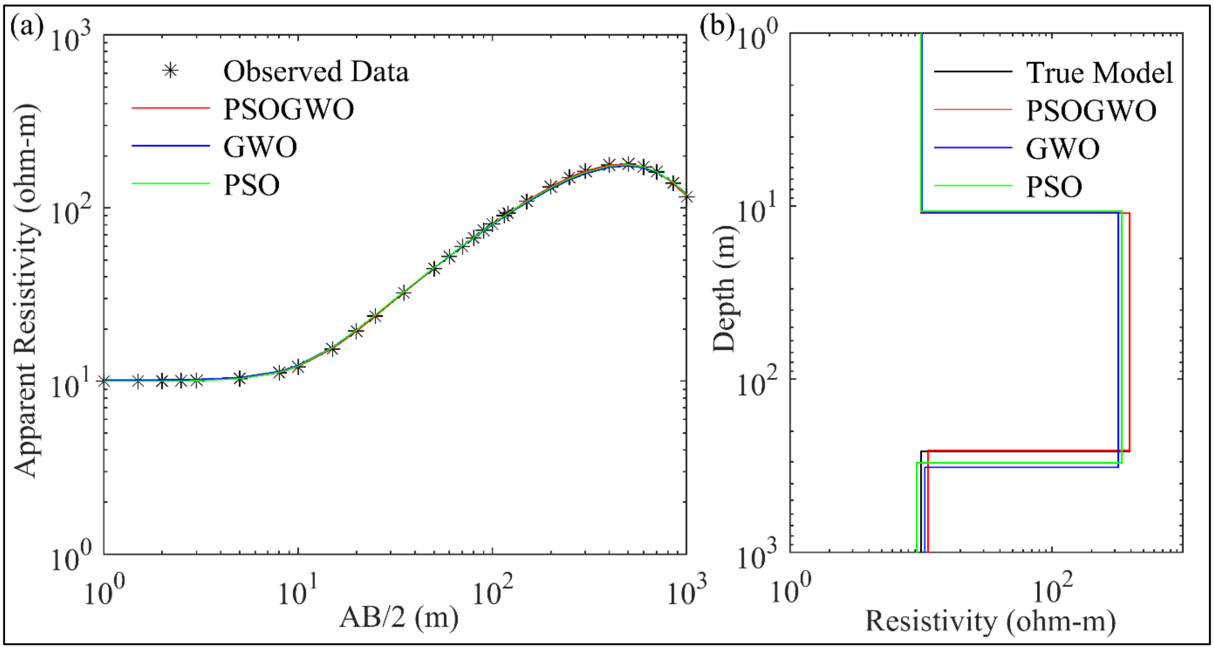

Figure 2. Three layer synthetic data (a) observed (*) and the best fitted calculated apparent resistivity curve (> 68.27% PDF); (b) one dimensional mean model (> 68.27% PDF) for true model (black colour), vPSOGWO (red colour), GWO (blue colour) and PSO (green colour).

The search limit for novel inversions techniques (vPSOGWO, GWO, and PSO) is carefully chosen, as shown in *Table 1*. Each algorithm, including vPSOGWO, runs 10,000 times to perform statistical analysis and determine the global mean model with the least uncertainty. *Fig. 3* shows the convergence curve of the resistivity layer parameters using vPSOGWO. We found no changes seen in the convergence pattern after 590 iterations, and layer parameters get stable. The convergence curves in terms of error versus iterations for existed three algorithms are shown in *Fig. 4*. It is observed that vPSOGWO, GWO, and PSO have converged at 590, 950, and 380 iterations with the mean square error of 1.586e–8, 5.238e–8, and 5.792e–8, respectively, whereas ridge regression has an error of 0.633.

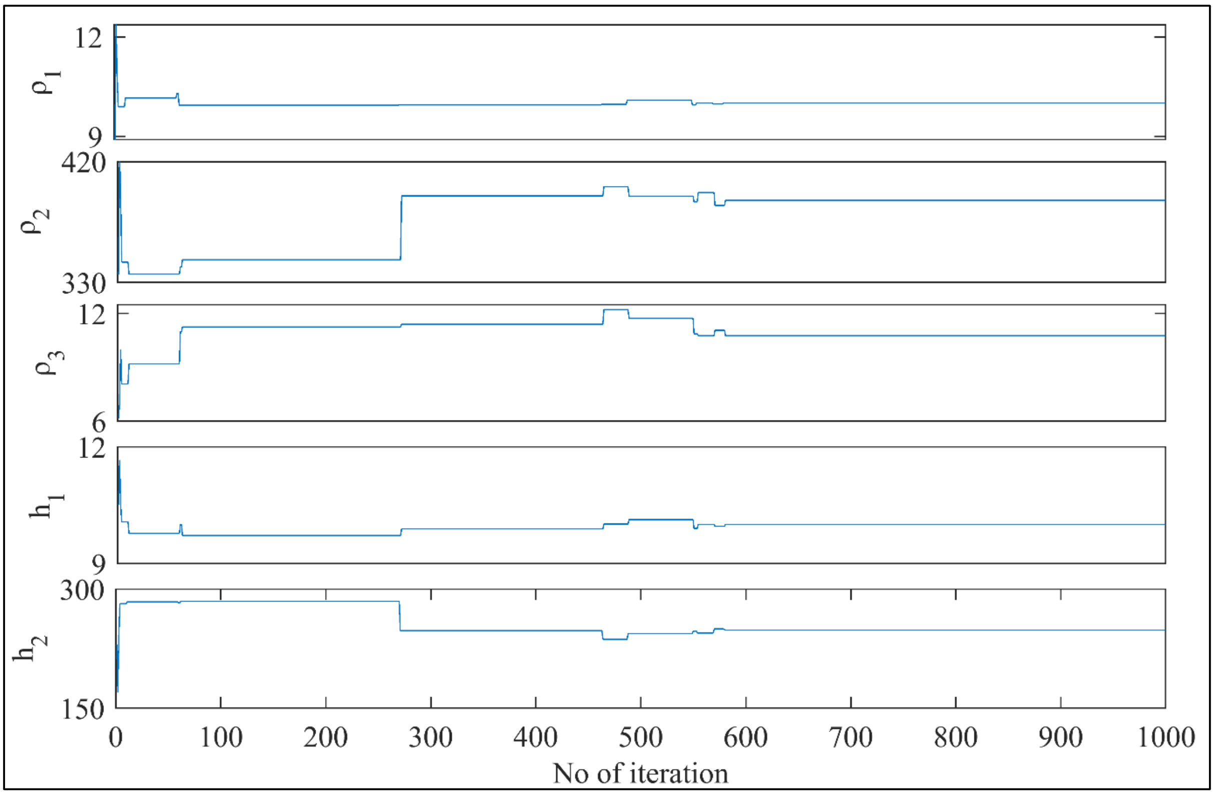

-

Figure 3. Convergence curve for best fitted model parameters for vPSOGWO algorithm.

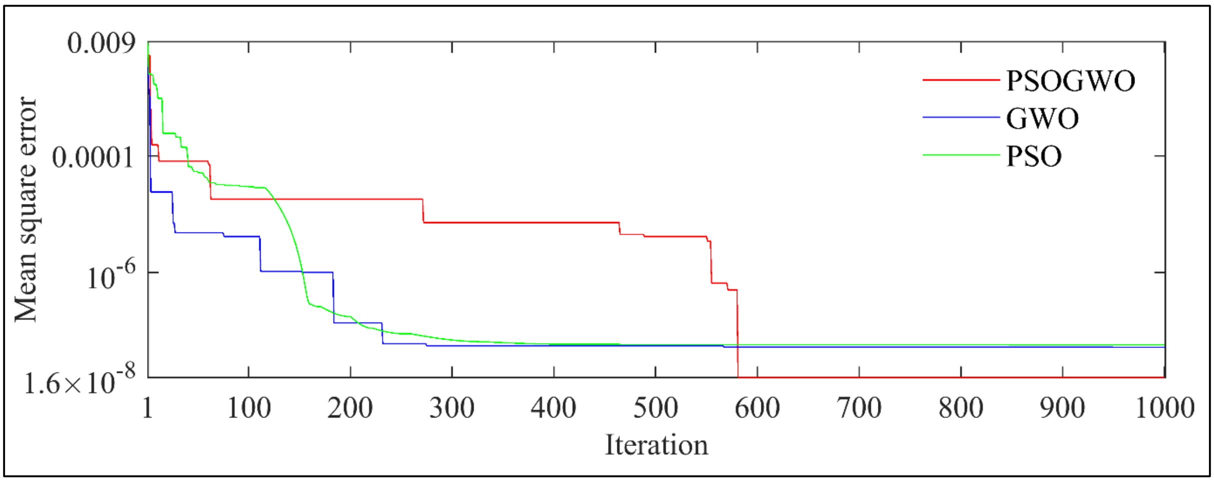

Figure 4. Convergent curve known as error versus iteration curve for three layers noiseless synthetic data.

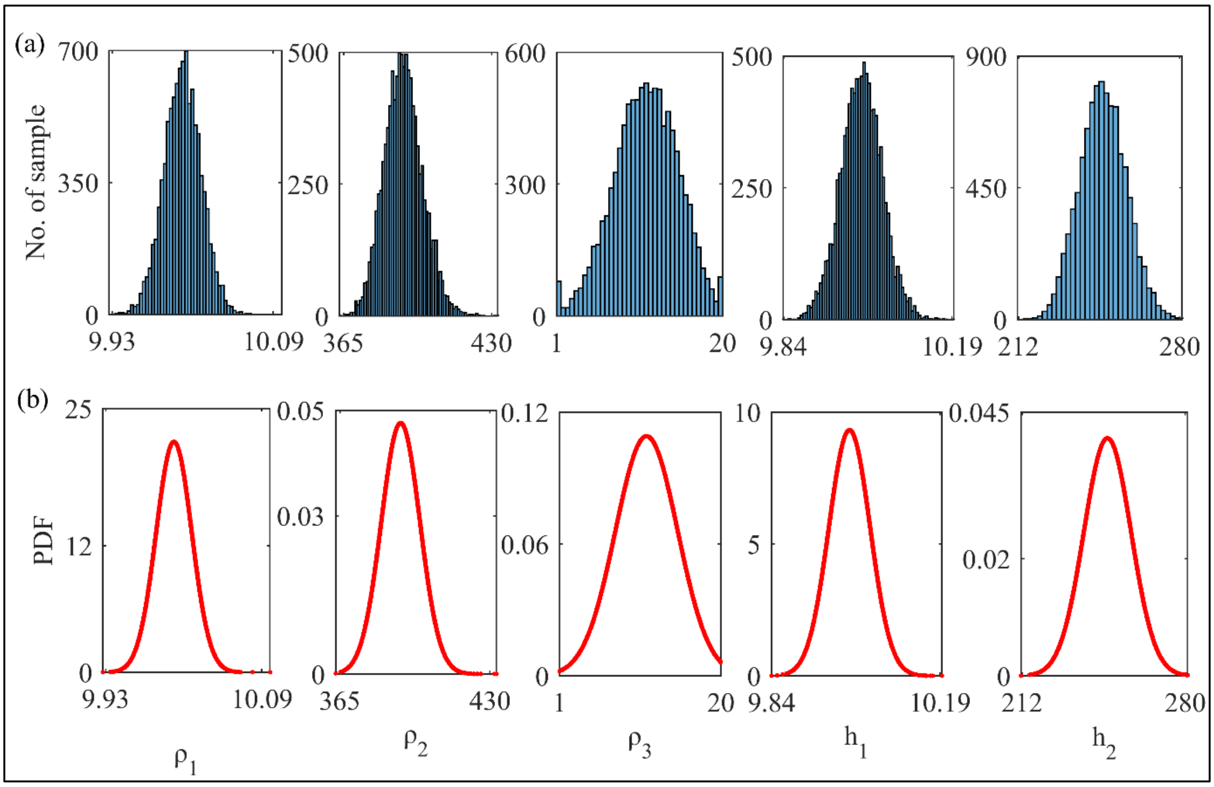

Figure 5. (a) Histogram and (b) posterior PDF of all 10,000 solution corresponding to output of each run for three layer synthetic earth model.

-

The 10,000 models inverted are used to find out the posterior PDF and histogram for each parameter. As shown in *Fig.* 5(a), the peak of posterior PDF is roughly close to the actual model parameter. The histogram is shown in *Fig. 5(b)* suggests that the ρ_2 and h_2 have a broader range. It represents the equivalence problem associated with the resistive layer as the uncertainty in each algorithm was found to be large considering all the accepted models. So by selecting the models having posterior PDF greater than 68.27% CI reduces the uncertainty in the model, increases the resolution of a solution, and helps estimate the best mean model close to the actual model (*Table 1)*. *Table 1* shows the model parameters and uncertainty for proposed algorithms.

Table 1. Optimization mean model result for three layer synthetic resistivity sounding data.

Model Parameter	True value	Search Range	Inman (1975)	Mean model (final 10000 sol.)			Mean model (PDF > 68.27%)		
				GWO	PSO	vPSOGWO	GWO	PSO	vPSOGWO
$\rho 1$ (Ωm)	10	5 – 15	10 ± 0.06	10.33 ± 0.55	10 ± 0.39	10 ± 0.02	10.15 ± 0.23	9.98 ± 0.08	10 ± 0.01
$\rho 2$ (Ωm)	390	15 – 500	398 ± 8.2	324.55 ± 56.71	343.10 ± 49.70	391.29 ± 8.39	319.15 ± 24.02	340.90 ± 23.10	391.09 ± 3.67
$\rho 3$ (Ωm)	10	1 – 20	10 ± 0.05	10.50 ± 3.76	9.56 ± 7.78	11.25 ± 3.66	10.71 ± 1.88	9.25 ± 2.84	11.27 ± 1.70
h1 (m)	10	1 – 20	10.1 ± 0.09	10.15 ± 0.82	9.74 ± 0.56	10 ± 0.04	9.85 ± 0.33	9.72 ± 0.18	10 ± 0.02
h2 (m)	250	100 – 500	245 ± 4.9	314.70 ± 61.46	299.55 ± 54.63	247.59 ± 9.84	312.61 ± 26.91	293.21 ± 23.57	247.51 ± 3.93

Here, two approaches are used to present the mean solution with its uncertainty estimation: (i) the mean solution for all accepted best-fitted solutions obtained from 10,000 runs for all three algorithms; and (ii) the mean model calculated from solution with posterior PDF, which values are greater than 68.27% CI from all accepted solution parameters.

-

Table 2. Correlation matrix using 68.27% PDF limit for three layer synthetic resistivity sounding data.

Model Parmeter	ρ1 (Ωm)	ρ2 (Ωm)	ρ3 (Ωm)	h1 (m)	h2 (m)
ρ1 (Ωm)	1.0000	–0.0575	0.0142	0.3820	0.0222
ρ2 (Ωm)		1.0000	0.2585	0.6293	–0.7994
ρ3 (Ωm)			1.0000	0.0537	–0.7678
h1 (m)				1.0000	–0.4278
h2 (m)					1.0000

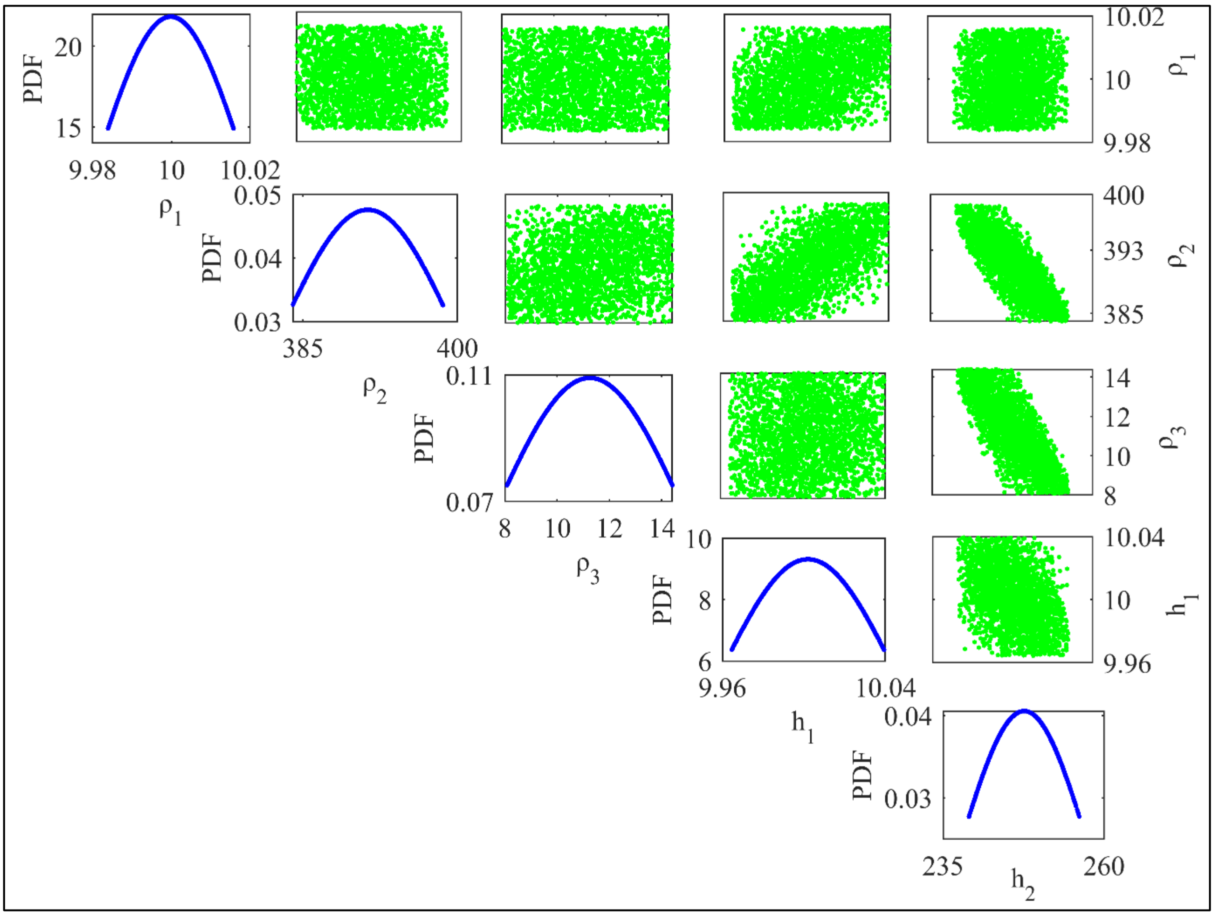

Figure 6. Correlation plot between model parameters (off diagonal) and posterior PDF curve (diagonal) from models having all parameters greater than 68.27% PDF.

Here, we observed that the second layer parameters for PSO and GWO are too diverted from actual values with higher uncertainty due to their inability to balance

-

exploitation and exploration properties. In contrast, the hybrid vPSOGWO algorithm provides more accurate results and falls within its uncertainty ranges (*Table 1)*. Therefore, a hybrid algorithm has better exploitation and exploration balancing nature than PSO and GWO. As shown in *Table 2*, the posterior correlation matrix illustrations that first layer resistivity reveals a feeble correlation with other associated parameters. Whereas there is a negative correlation found between ρ_2 and h_2, both parameters have a trade-off relationship.

In contrast, a positive correlation between ρ_2 and h_1 is observed (i.e., resistivity of the second layer increases with increasing the thickness of the first layer and vice versa). Similarly, it can also be seen between third layer resistivity and second layer thickness but inverse in nature. *Fig. 6* represents the correlation plot between model parameters (off-diagonal) with the posterior PDF curve (diagonal) for models greater than 68.27% CI for all parameters. No significant error differences are found between the observed and calculated apparent resistivity data for all three algorithms (*Fig. 2(a))*. However, the error difference in the 1D model and result for 68.27% CI's mean model are presented in *Fig. 2(b) and Table 1*, respectively.

Table 3. Stability test for three layer synthetic resistivity sounding data using different search range.

Model Parameter	ρ1 (Ωm)	ρ2 (Ωm)	ρ3 (Ωm)	h1 (m)	h2 (m)
True values	10	390	10	10	250
Search Range	5 - 30	500 – 1000	15 – 30	1 – 10	50 – 90
vPSOGWO	10 ± 0.02	390.44 ± 8	10.48 ± 3.60	10 ± 0.04	249.25 ± 9.93
Search Range	2.5 - 30	7.5 – 750	0.1 – 40	1 – 40	50 - 750
vPSOGWO	10 ± 0.03	398.39 ± 18.01	15.93 ± 8.47	10.02 ± 0.07	237.24 ± 21.98
Search Range	1 - 60	1 – 1000	0.01 – 80	1 - 80	1 - 1000
vPSOGWO	10 ± 0.03	428.11 ± 60.40	23.14 ± 13.19	10.10 ± 0.15	214.86 ± 39.66

-

To check the stability of the parameter, the hybrid algorithm is tested with three different search spaces, as shown in *Table 3*. Consequently, it estimates the mean model and uncertainty for 100 runs. This Table illuminates using a broader search space suggests that the result does not divert too much from the actual model. The computations time required for vPSOGWO, GWO, and PSO are 1.54s, 1.49s, and 1.48s, respectively, for one run with 30 data points in this example.

Table 4. Optimization mean model result for three layer synthetic resistivity sounding data with 10% noise.

Model Parameter	True value	Search Range	Mean model (final 10000 sol.)			Mean model (PDF > 68.27%)		
			GWO	PSO	vPSOGWO	GWO	PSO	vPSOGWO
$\rho 1$ (Ωm)	10	5 – 15	10.37 ± 0.56	10.05 ± 0.40	10.04 ± 0.02	10.21 ± 0.24	10.03 ± 0.08	10.04 ± 0.01
$\rho 2$ (Ωm)	390	15 – 500	323.27 ± 55.51	341.58 ± 49.74	384.37 ± 7.78	317.68 ± 24.39	339.42 ± 23	384.24 ± 3.41
$\rho 3$ (Ωm)	10	1 – 20	10.46 ± 3.79	9.57 ± 7.78	11.17 ± 3.60	10.61 ± 1.94	9.35 ± 2.84	11.17 ± 1.65
h1 (m)	10	1 – 20	10.16 ± 0.83	9.75 ± 0.57	9.99 ± 0.04	9.89 ± 0.35	9.74 ± 0.18	9.99 ± 0.02
h2 (m)	250	100 – 500	314.65 ± 60.48	300 ± 54.45	251.72 ± 9.59	312.96 ± 27.59	293.61 ± 23.54	251.64 ± 3.82

The proposed optimization is also performed using the same synthetic data with 10% Gaussian noise and keeping the search range (*Table 1).* The same procedure is applied to determine the mean model from all best-fitted solutions and solutions with posterior PDF greater than 68.27% CI used for parameters of all the solutions (*Table 4).* Although a 10% noise is added, the result obtained from the mean model for posterior PDF of 68.27% for the hybrid algorithm is not much diverted from actual values. At the same time, the error was observed that slightly increase 1.309e–5, 1.313e–5, and 1.327e–5 for

-

vPSOGWO, GWO, and PSO, respectively. *Table 5* depicts the correlation matrix of the vPSOGWO, which clearly described interdependence by 0.3315 and –0.7879 for the first and second layer's parameters. Similarly, we can also determine the relation between second layer resistivity and first layer thickness (0.6142), third layer resistivity, and the second layer thickness (-0.7618). Hence, it shows good agreement with the actual model values.

Table 5. Correlation matrix using 68.27% PDF limit for three layer synthetic resistivity sounding data with 10% noise.

Model Parmeter	$\rho1$ (Ωm)	$\rho2$ (Ωm)	$\rho3$ (Ωm)	h1 (m)	h2 (m)
$\rho1$ (Ωm)	1.0000	–0.0816	–0.0017	0.3315	–0.0552
$\rho2$ (Ωm)		1.0000	0.2356	0.6142	–0.7879
$\rho3$ (Ωm)			1.0000	0.0064	–0.7618
h1 (m)				1.0000	–0.3922
h2 (m)					1.0000

6.2 Example 2: Synthetic data- Four layers case

The four-layer earth model having a thin, relatively low resistive (24.0 Ωm) sandwiched between the two high resistivity layers (840.0 Ωm and 8400.0 Ωm) is considered for demonstration of the proposed algorithms. *Table 6* illustrates the actual model for synthetic data, search range, and inverted results. The vPSOGWO, GWO, and PSO converge at iterations 590, 674, and 750 with associated errors 3.624e–8, 1.370e–8, and 2.097e–7, respectively as shown in *Fig. 8,* whereas the error estimated using ridge regression method is 0.383. Instead of higher error in vPSOGWO than GWO, it can also be observed that the error scale for the vPSOGWO algorithm is narrower than the other two algorithms, which is an essential factor for determining the mean model (*Fig. 9*). Hence, the mean model is affected by the error scale, as shown in *Fig. 9*.

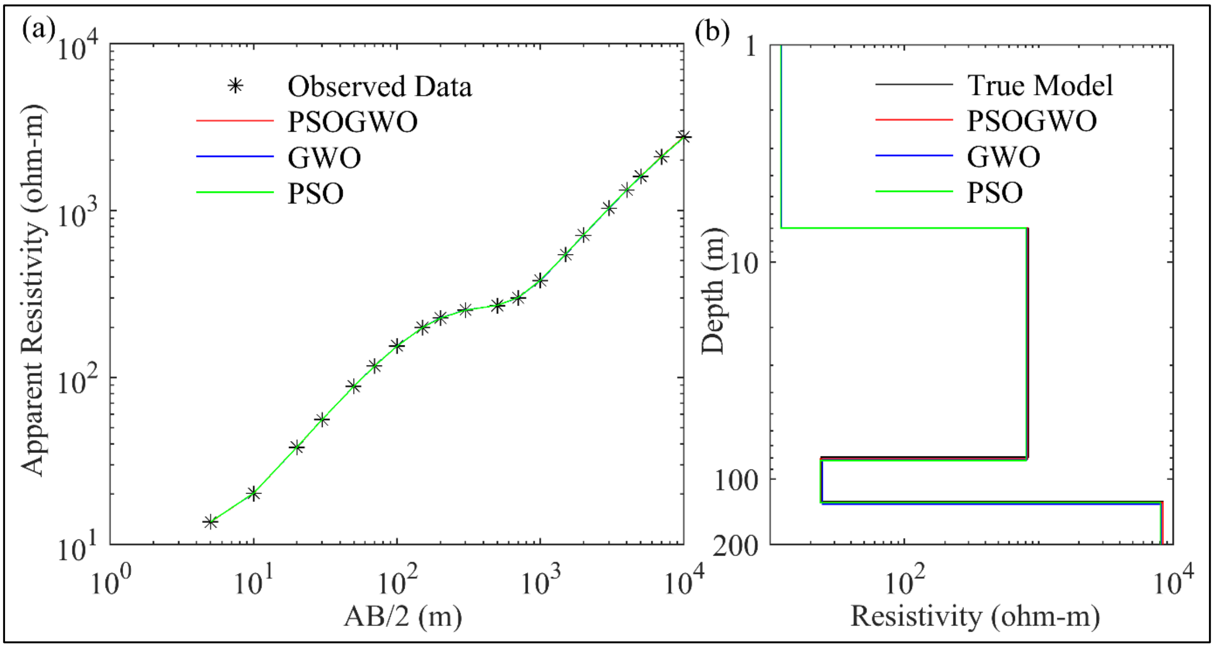

Figure 7. Four layer synthetic data: (a) observed (*) and the best fitted calculated apparent resistivity curve (> 68.27% PDF); (b) one dimensional mean model (> 68.27% PDF) for true model (black colour), vPSOGWO (red colour), GWO (blue colour) and PSO (green colour).

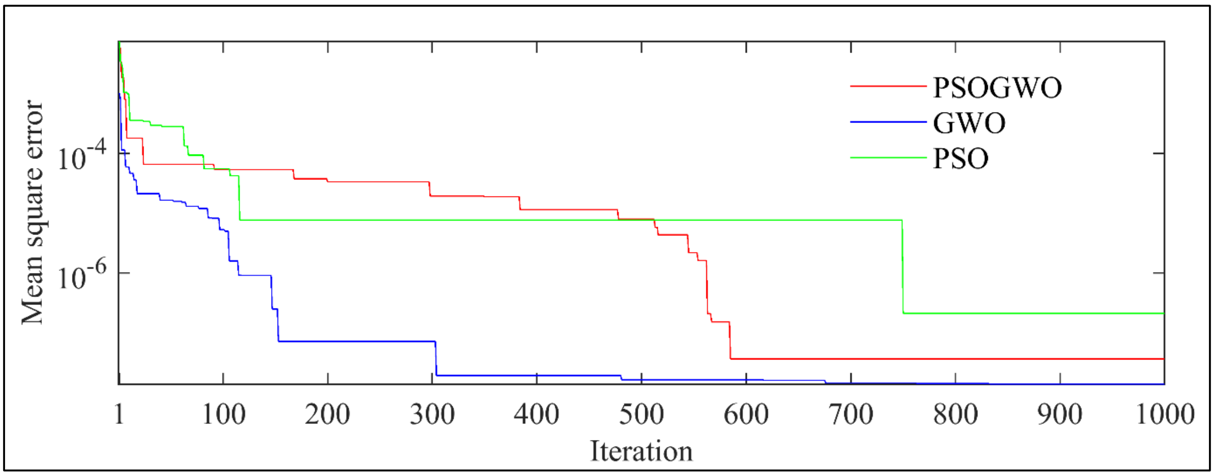

Figure 8. Convergent curve known as error versus iteration curve for four layers noiseless synthetic resistivity sounding data.

-

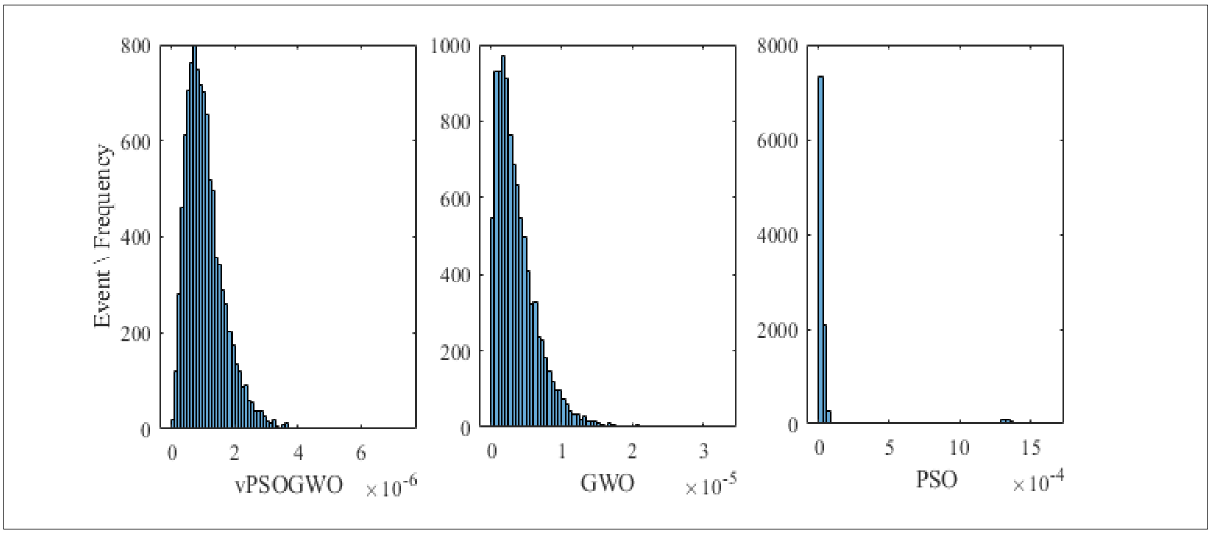

Figure 9. Histogram of logarithmic mean square error for vPSOGWO, GWO and PSO over 10,000 models. The x axis of three histogram represent the misfit error correspond to 10,000 models.

Table 6. Optimization mean model result for four layer synthetic resistivity sounding data.

Model Parameter	True value	Search Range	Ridge regression (Inman, 1975)	Mean model (final 10000 sol.)			Mean model (PDF > 68.27%)		
				GWO	PSO	vPSOGWO	GWO	PSO	vPSOGWO
ρ1 (Ωm)	12	5 – 30	12.1 ± 0.1	12.03 ± 0.07	12.10 ± 1.05	11.99 ± 0.08	12.02 ± 0.03	12.01 ± 0.39	11.99 ± 0.04
ρ2 (Ωm)	840	500 – 1000	814 ± 62	809.16 ± 28.80	802.90 ± 69.13	824.36 ± 58.13	814.38 ± 10.86	803.12 ± 31.07	822.71 ± 26.06
ρ3 (Ωm)	24	15 – 30	18.2 ± 805	24.34 ± 1.30	23.78 ± 5.01	23.59 ± 3	24.50 ± 0.36	23.50 ± 1.95	23.69 ± 1.41
ρ4 (Ωm)	8400	5000 – 10000	7500 ± 3275	8151.4 ± 293.68	8068.1 ± 614.66	8415.50 ± 151.53	8150.1 ± 118.05	8065.2 ± 301.79	8411.9 ± 70.40
h1 (m)	6	1 – 10	6 ± 0.07	6 ± 0.06	6.04 ± 0.68	5.99 ± 0.06	6 ± 0.03	5.99 ± 0.22	5.99 ± 0.03
h2 (m)	72	50 – 90	74 ± 25.7	75.13 ± 2.82	75.79 ± 7.36	73.99 ± 5.71	74.61 ± 0.94	75.14 ± 3.20	73.77 ± 2.59
h3 (m)	48	30 – 60	36 ± 1595	48.43 ± 2.71	46.98 ± 9.93	47.10 ± 5.98	48.82 ± 0.88	46.46 ± 3.86	47.30 ± 2.81

To reduce uncertainty and increase the resolution of the model, model parameters containing posterior PDF greater than 68.27% CI are selected. In *Table 6*, the true model lies within the uncertainty range of hybrid vPSOGWO, whereas GWO and PSO have failed to keep the true model within its uncertainty range in the second, third, and fourth layer's parameters. In the case of ridge regression, the uncertainty level of the model parameters is too high. For example, in the case of the third layer, both resistivity and thickness have uncertainty approx. 44 times higher than the actual value.

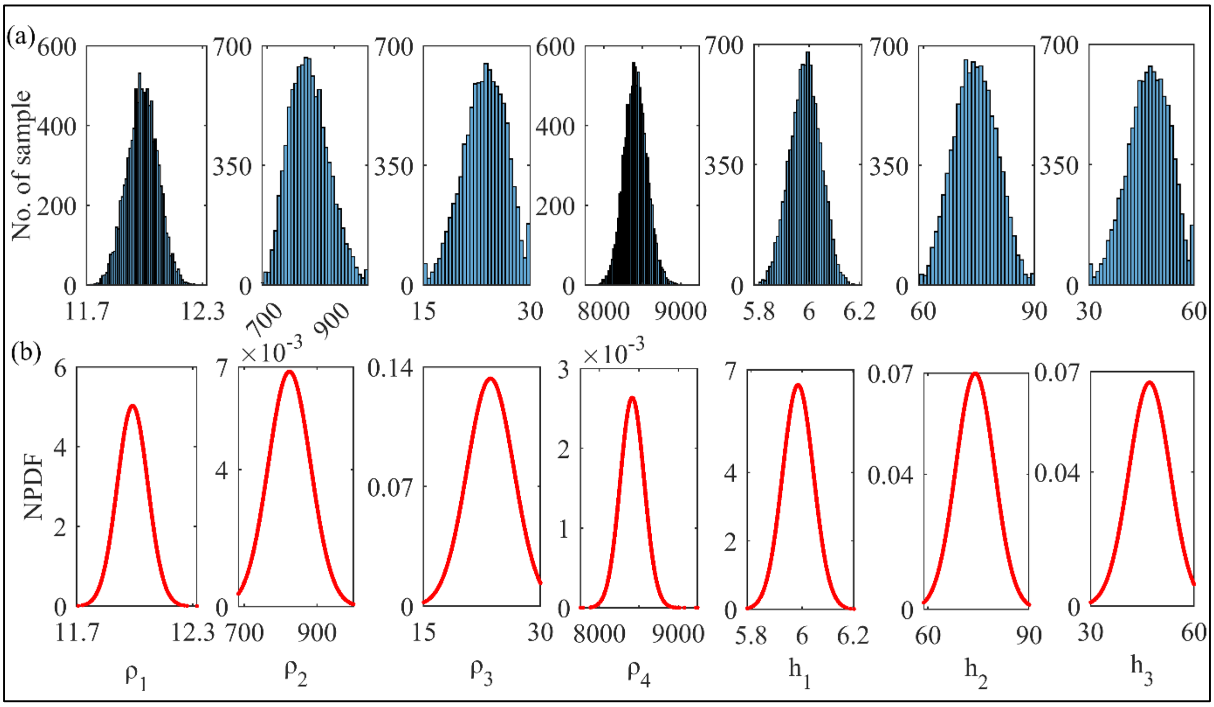

Figure 10. (a) Histogram and (b) posterior PDF of all 10,000 solution corresponding to output of each run for four layer synthetic resistivity sounding data.

The inverted 10,000 models are also computed in this example to find out the posterior PDF and histogram for each parameter. The peak of posterior PDF is roughly nearby the actual solution, as shown in histogram *Fig. 10(a) and Fig. 10(b) reveals* the ρ_2 and h_2 have a broader range that signifies the equivalence problem associated with the resistive layer. The uncertainty in each algorithm is found to be large considering all the accepted models. However, picking the models with greater posterior PDF than 68.27% CI reduces the uncertainty in the model, increases the resolution of a solution.

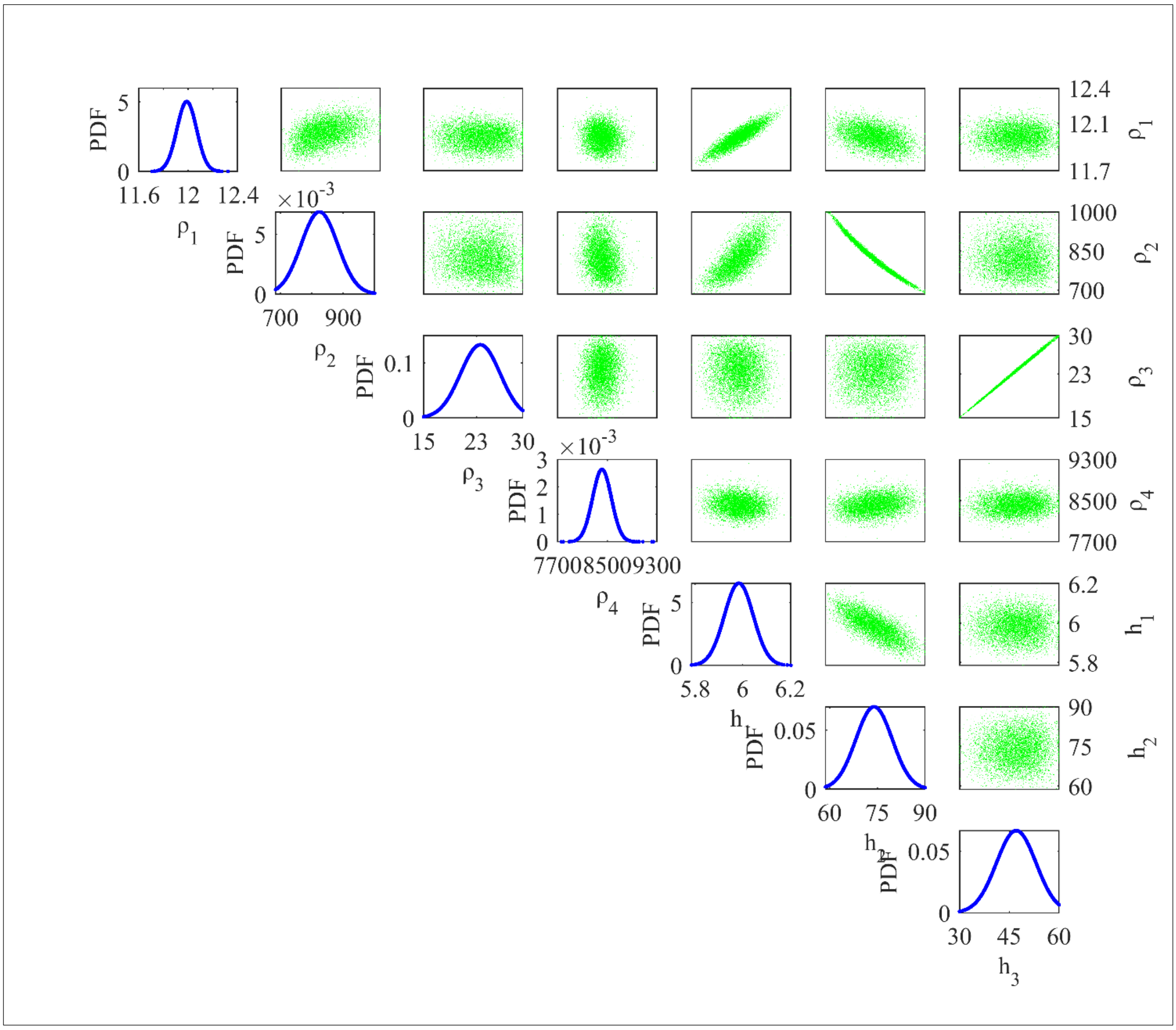

Figure 11. Correlation plot between model parameters (off diagonal) and posterior PDF curve (diagonal) from models having all parameters greater than 68.27% PDF.

The correlation plot between model parameters (off-diagonal) with the posterior PDF curve (diagonal) for models greater than 68.27% CI for all parameters is shown in *Fig. 11*. There are also no significant error differences between the computed and observed apparent resistivity data for all three optimization algorithms.

-

Table 7. Correlation matrix using 68.27% PDF limit for four layer synthetic resistivity sounding data.

Model Parmeter	ρ1 (Ωm)	ρ2 (Ωm)	ρ3 (Ωm)	ρ4 (Ωm)	h1 (m)	h2 (m)	h3 (m)
ρ1 (Ωm)	1.0000	–0.0359	–0.0029	–0.0207	0.7383	0.0354	–0.0041
ρ2 (Ωm)		1.0000	–0.0481	–0.0598	0.4667	–0.9798	–0.0105
ρ3 (Ωm)			1.0000	0.0284	–0.0188	0.0274	0.9983
ρ4 (Ωm)				1.0000	–0.0183	0.0935	0.0509
h1 (m)					1.0000	–0.4286	–0.0036
h2 (m)						1.0000	–0.0079
h3 (m)							1.0000

The correlation matrix of a four-layer model of synthetic resistivity data is shown in *Table 7*. It illustrations that the first layer parameters are correlated by a correlation matrix of 0.7383. A strong negative correlation was found between the second layer parameters (-0.9798), and the third layer parameters are strongly correlated with each other by a positive correlation matrix of 0.9983. *Fig. 7(a)* shows the fitness between four-layer synthetic (*) and computed apparent resistivity data obtained for vPSOGWO, GWO, and PSO. The difference in fitness curves for all three optimization techniques cannot be determined as the observed error is significantly negligible. However, the error difference can be observed in the 1D resistivity-depth models obtained from 68.27% CI's mean model, as shown in *Fig. 7(b)*. *Table 6* shows the mean model having posterior PDF greater than 68.27% CI for all accepted parameters in the four-layer earth model case. The computation time for vPSOGWO, GWO, and PSO are 1.94s, 1.84s, and 1.85s (PSO), respectively, for one run with 27 data points in this example.

The optimization techniques are also executed using the same four-layer model of synthetic data with 10% Gaussian noise and keeping the search range in *Table 6*. The same

-

procedure is applied to determine the mean model from all the best-fitted models and models of a posterior PDF greater than 68.27% CI for all model parameters presented in *Table 8*. Although a 10% noise is added, the result obtained from the mean model for the posterior PDF of 68.27% for the hybrid algorithm is not much diverted from actual values. At the same time, the experimental error is 3.831e–4, 3.831e–4, and 3.870e–4 for vPSOGWO, GWO, and PSO, respectively.

Table 8. Optimization mean model result for four layer synthetic resistivity sounding data with 10% noise.

Model Parameter	True value	Search Range	Mean model (final 10000 sol.)			Mean model (PDF > 68.27%)		
			GWO	PSO	vPSOGWO	GWO	PSO	vPSOGWO
$\rho 1$ (Ωm)	12	5 - 30	12.25 ± 0.07	12.38 ± 1.03	12.27 ± 0.09	12.24 ± 0.03	12.26 ± 0.37	12.27 ± 0.04
$\rho 2$ (Ωm)	840	500 – 1000	813.70 ± 31.51	816.76 ± 66.79	901.03 ± 53.95	812.08 ± 12.36	816.46 ± 29.21	899.24 ± 24.66
$\rho 3$ (Ωm)	24	15 - 30	24.17 ± 1.36	23.51 ± 5.03	23.59 ± 2.84	24.31 ± 0.42	23.28 ± 1.87	23.50 ± 1.37
$\rho 4$ (Ωm)	8400	5000 - 10000	8070.5 ± 310.96	7971.2 ± 596.07	8415.50 ± 167.11	8082 ± 143.09	7973.5 ± 292.28	8417 ± 80.27
h1 (m)	6	1 - 10	6.15 ± 0.06	6.22 ± 0.67	5.99 ± 0.06	6.15 ± 0.03	6.15 ± 0.21	6.20 ± 0.03
h2 (m)	72	50 - 90	76.80 ± 2.98	76.96 ± 6.96	73.99 ± 4.59	76.72 ± 1.29	76.38 ± 3.00	69.75 ± 2.10
h3 (m)	48	30 - 60	47.35 ± 2.84	47.35 ± 10.09	47.10 ± 5.85	48.75 ± 0.94	47.02 ± 3.77	48.27 ± 2.83

Table 9 illustrates the correlation matrix of the hybrid algorithm, which clearly described interdependence by 0.7644, –0.9665, and 0.9980 for the first and second, and third layers parameters. Similarly, we can also find out the relation between second layer resistivity and first layer thickness (0.3605) and the resistivity of the fourth layer and thickness of the third layer (0.0549). Hence, it shows good agreement with the actual model values.

-

Table 9. Correlation matrix using 68.27% PDF limit for four layer synthetic resistivity sounding data with 10% noise.

Model Parmeter	ρ1 (Ωm)	ρ2 (Ωm)	ρ3 (Ωm)	ρ4 (Ωm)	h1 (m)	h2 (m)	h3 (m)
ρ1 (Ωm)	1.0000	0.0003	0.0271	–0.0948	0.7644	–0.0109	0.0251
ρ2 (Ωm)		1.0000	–0.0168	0.0327	0.3605	–0.9665	0.0153
ρ3 (Ωm)			1.0000	0.0260	0.0211	–0.0042	0.9980
ρ4 (Ωm)				1.0000	–0.0446	0.0009	0.0549
h1 (m)					1.0000	–0.3180	0.0268
h2 (m)						1.0000	–0.0329
h3 (m)							1.0000

6.3 Example 3: Field data - Three-layer case

We have taken one three-layer case of vertical electrical resistivity sounding data measured with Schlumberger array over Mt. Turner, North Queensland, Australia, interpreted by Dixon and Doherty (1977, *Fig. 2a*), as shown in *Fig. 12(a)*. After selecting a suitable search range, three novel algorithms, namely vPSOGWO, GWO, and PSO, are executed to reconstruct the model interpreted by Dixon and Doherty (1977). The search range and comparison among proposed algorithms with the previous result (Dixon and Doherty, 1977) are presented in *Table 10*. Our results (for 68.27% CI) are closed to the development given by Dixon and Doherty (1977). The convergent error for the best-fitted model in vPSOGWO is 3.681e–4, whereas GWO is 3.697e–4, and PSO is 3.682e–4.

-

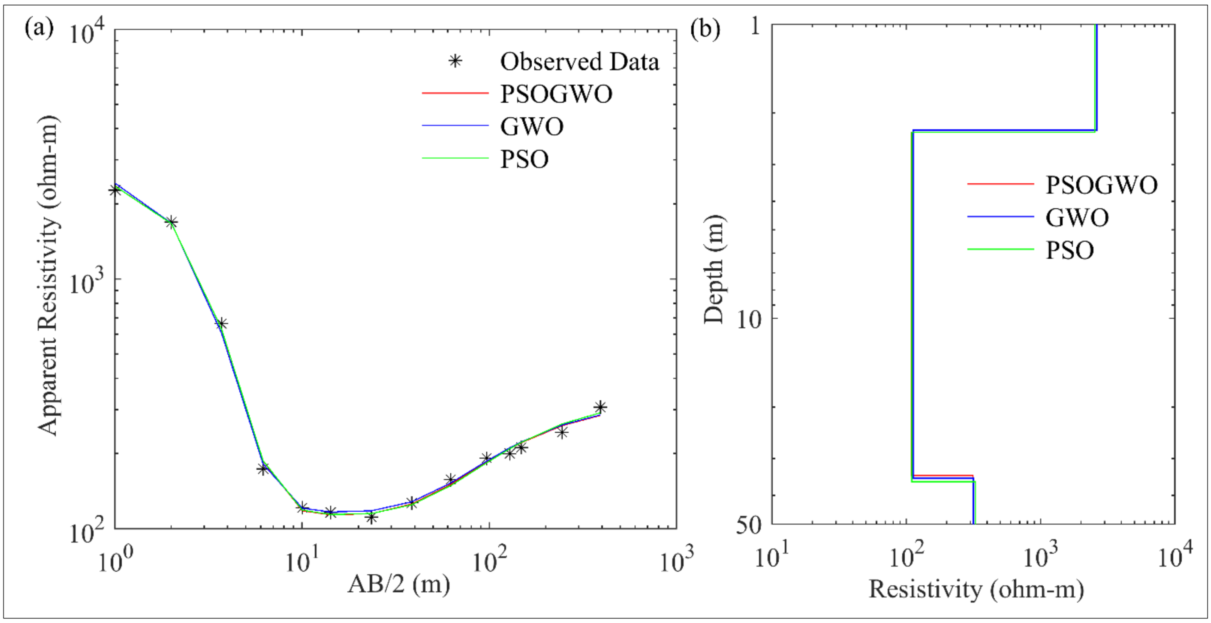

Figure 12. Three layer field data over Mt. Turner, North Queenland, Australia: (a) observed (*) and the best fitted calculated apparent resistivity curve (> 68.27% PDF); (b) one dimensional mean model (> 68.27% PDF) for true model (black colour), vPSOGWO (red colour), GWO (blue colour) and PSO (green colour).

Table 10. Optimization mean model result for three layer field resistivity sounding data.

Model Parameter	Search Range	Dixon and Doherty (1977)	Mean model (final 10000 sol.)			Mean model (PDF > 68.27%)		
			GWO	PSO	vPSOGWO	GWO	PSO	vPSOGWO
$\rho1$ (Ωm)	2000 – 3000	2500	2646.6 ± 246.65	2532.3 ± 78.20	2536 ± 8.67	2619.8 ± 109.70	2533.8 ± 34.59	2535.9 ± 4.05
$\rho2$ (Ωm)	10 – 400	100	116.01 ± 16.45	110.17 ± 3.38	109.23 ± 0.29	112.55 ± 4.65	109.78 ± 1.11	109.24 ± 0.13
$\rho3$ (Ωm)	200 – 500	300	318.99 ± 31.67	334.01 ± 33.22	314.42 ± 1.63	315.50 ± 11.96	327.15 ± 14.93	314.40 ± 0.77
h1 (m)	0.1 – 3	1.42 (approx.)	1.28 ± 0.13	1.33 ± 0.02	1.33 ± 0.00	1.29 ± 0.05	1.33 ± 0.01	1.33 ± 0.00
h2 (m)	20 - 50	29.21 (approx.)	34.02 ± 7.38	34.91 ± 6.29	31.90 ± 0.31	32.66 ± 2.99	33.67 ± 2.17	31.90 ± 2.17

-

Table 11. Correlation matrix using 68.27% PDF limit for three layer field resistivity 535 sounding data.

Model Parmeter	$\rho 1$ (Ωm)	$\rho 2$ (Ωm)	$\rho 3$ (Ωm)	h1 (m)	h2 (m)
$\rho 1$ (Ωm)	1.0000	0.0046	–0.0003	–0.2336	0.0086
$\rho 2$ (Ωm)		1.0000	–0.0389	–0.0897	0.3075
$\rho 3$ (Ωm)			1.0000	0.0144	0.4050
h1 (m)				1.0000	–0.0256
h2 (m)					1.0000

Table 11 presents the correlation matrix, which shows a negative correlation between the first layer parameters, and a positive correlation is observed between the second layer parameters. A positive correlation is also observed between ρ_3 and h_2, which maintains the same model data. *Fig. 12(a)* shows the apparent resistivity curve and the 1D model obtained from the mean model with a 68.27% CI result shown in *Fig. 12(b)*. The computation time requires for one run in this example with 14 data points is 0.90s (vPSOGWO), 0.83s (GWO), and 0.78s (PSO), respectively.

6.4 Example 4: Field data - Five-layer case

We have selected another field example using a vertical electrical resistivity sounding data as a five-layer case of earth's subsurface model from Keshiari-Kharagpur near Kharagpur, West Bengal, India, to determine the aquifer zone (Panda et al., 2018, *Fig. 3*). The area is covered with different geological units such as laterite, clay, sand, etc., and laterite material restricts the aquifer's recharge process and most problematic area for groundwater potential. We inverted this data for a five-layered earth structure parameter using the vPSOGWO, GWO, and PSO inversion algorithm. The results are shown in *Table 12* available model, borehole sample, and the search space for vPSOGWO, GWO, and PSO.

-

The computed apparent resistivity curve for all the three algorithms (-) and field data indicated by the symbol (*) are shown in *Fig. 13(a)*. Their error differences are significant (*Fig. 13a, Table 12*). The inverted 1D layered model using all algorithms obtained from 68.27% CI's mean model is shown in *Fig. 13(b)*. The computations time for vPSOGWO, GWO, and PSO are 2.55s, 2.43s, and 2.45s, respectively, for one run with 28 data points in this example.

Table 12. Optimization mean model result for five layer field resistivity sounding data.

Model Parameter	Search Range	Litho log detail of 100m deep	VES6 (Panda et al., 2017) VFSA	Mean model (final 10000 sol.)			Mean model (PDF > 68.27%)		
				GWO	PSO	vPSOGWO	GWO	PSO	vPSOGWO
$\rho 1$ (Ωm)	60 – 120	- -	97 ± 5	87.97 ± 10.02	88.41 ± 13.73	78.21 ± 8.28	87.44 ± 3.37	88.43 ± 5.31	77.99 ± 3.17
$\rho 2$ (Ωm)	10 – 30	- -	19 ± 0.2	20.38 ± 0.87	19.38 ± 1.18	19.73 ± 0.17	20.43 ± 0.34	19.43 ± 0.43	19.73 ± 0.06
$\rho 3$ (Ωm)	80 - 150	- -	128 ± 29	116.04 ± 10.01	118.34 ± 14.41	123.24 ± 9.56	115.28 ± 3.50	117.55 ± 5.67	123.01 ± 3.67
$\rho 4$ (Ωm)	10 - 25	- -	60 ± 1	16.79 ± 1.31	15.27 ± 2.12	14.83 ± 0.69	16.93 ± 6.49	15.35 ± 0.83	14.84 ± 0.27
$\rho 5$ (Ωm)	25 -60	- -	40 ± 0.4	41.91 ± 2.99	44.46 ± 3.60	42.83 ± 0.52	41.61 ± 1.06	44.28 ± 1.35	42.67 ± 0.20
h1 (m)	0.2 – 0.9	0.6 (Dry soil)	0.5 ± 0.1	0.54 ± 0.05	0.56 ± 0.06	0.56 ± 0.02	0.53 ± 0.02	0.56 ± 0.02	0.56 ± 0.01
h2 (m)	5 – 10	7 (Moist soil)	6.5 ± 0.3	7.06 ± 0.56	6.35 ± 1.01	7.06 ± 0.13	7.10 ± 0.21	6.36 ± 0.35	7.06 ± 0.05
h3 (m)	6 – 10	8 (Compact laterite)	7.7 ± 2.3	8.41 ± 0.72	8.78 ± 1.33	8.37 ± 0.68	8.38 ± 0.26	8.77 ± 0.53	8.37 ± 0.26
h4 (m)	40 – 55	48 (Soft laterite)	45.0 ± 5.0	51.15 ± 3.57	48.34 ± 6.10	48.22 ± 3.28	51.37 ± 1.37	48.60 ± 2.42	48.23 ± 1.27

* The symbol "- -" in table stand for no information.

-

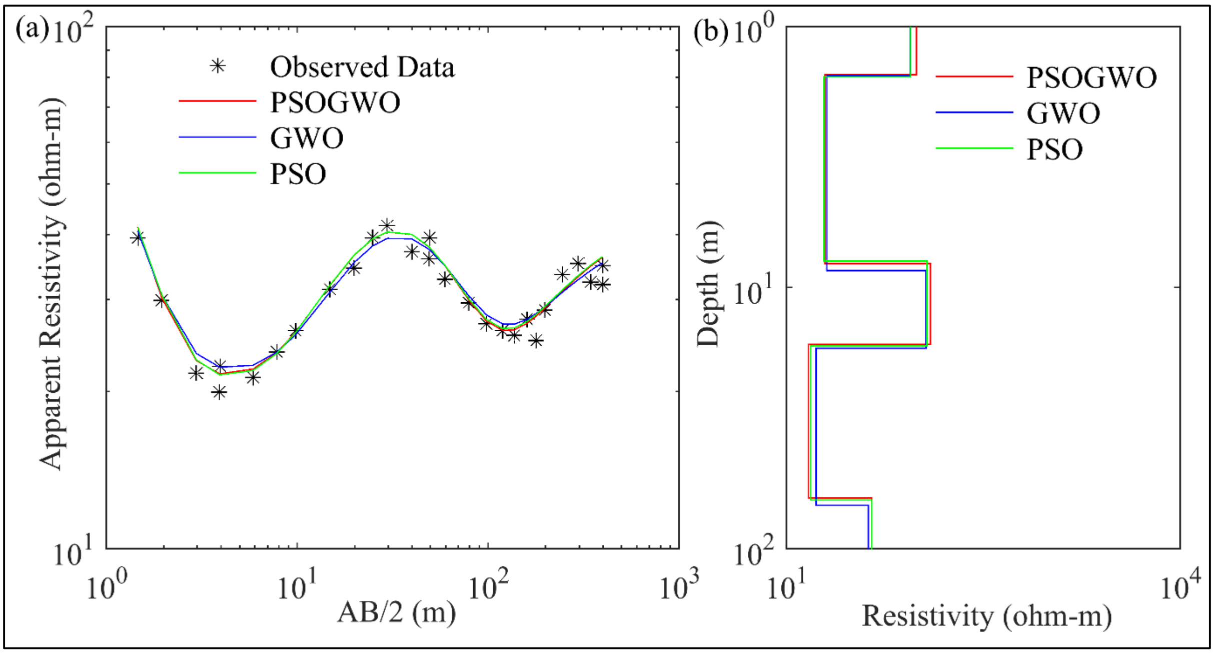

Figure 13. Five layer field data: (a) observed (*) and the best fitted calculated apparent resistivity curve (> 68.27% PDF); (b) one dimensional mean model (> 68.27% PDF) for true model (black colour), vPSOGWO (red colour), GWO (blue colour) and PSO (green colour).

Table 13. Correlation matrix using 68.27% PDF limit for five layer field resistivity sounding data.

Model Parmeter	$\rho1$ (Ωm)	$\rho2$ (Ωm)	$\rho3$ (Ωm)	$\rho4$ (Ωm)	$\rho5$ (Ωm)	h1 (m)	h2 (m)	h3 (m)	h4 (m)
$\rho1$ (Ωm)	1.0000	0.8103	0.0246	0.0164	0.1051	–0.9779	0.5888	–0.0288	0.0492
$\rho2$ (Ωm)		1.0000	0.1267	–0.1124	0.0684	–0.8652	0.7855	–0.1035	–0.0675
$\rho3$ (Ωm)			1.0000	–0.1272	–0.1221	–0.0390	0.6185	–0.9664	–0.1169
$\rho4$ (Ωm)				1.0000	0.4706	0.0028	–0.3107	–0.0985	0.9726
$\rho5$ (Ωm)					1.0000	–0.1026	–0.0414	0.0449	0.6416
h1 (m)						1.0000	–0.6356	0.0392	–0.0328
h2 (m)							1.0000	–0.5463	–0.2534
h3 (m)								1.0000	–0.0936
h4 (m)									1.0000

-

The result obtained from the mean solution of all accepted solutions and solutions with PDF greater than 68.27% CI aimed at all parameters using the developed techniques is presented in *Table 12*. The final mean models are comparable with lithological data of 100m deep tube well near VES6. The convergent error for vPSOGWO, GWO, and PSO are 4.498e–4, 4.541e–4, and 4.566e–4, respectively, whereas the error is 1.7e–2 for VFSA obtained by Panda et al. (2018). The correlation matrix clarifies a strong correlation between the parameters of the first layer (–0.9736), the second layer (0.8434), and the third layer (–0.9907) and a moderate relation between the parameters of the fourth layer (0.5653). We have noticed a moderate interdependence between ρ_3 with h_2 and ρ_5 with h_4, which follows to retain the same model data shown in *Table 13*.

6.5 Example 5: Field data - Six layer case

We again applied the vPSOGWO, GWO, and PSO algorithms to invert the field apparent resistivity data as a six-layer case study extracted near a borehole from in Apulia, South Italy, for hydrogeological purposes (Sen et al. 1993). The search range has been taken from Sen et al. (1993), but the fourth and upper bound thickness of the fifth layers increases by 50 m, as shown in *Table 14*. The reproduced field data (*) and inverted field data (-) are shown in *Fig. 14(a)*. The misfit error obtained is 2.830e–4, 3.243e–4, and 3.133e–4 for vPSOGWO, GWO, and PSO, respectively, whereas the error using Simulating Annealing (SA) is 0.017 by Sen et al. (1993). *Table 14* also includes the mean model for 100% and 68.27% CI using proposed algorithms and previously published literature. It is observed that few parameters obtained fall within the uncertainty of corresponding parameters of vPSOGWO. The vPSOGWO inverted results provide higher similarity with the borehole information than the results by SA (Sen et al., 1993). The interdependence between the layer parameter can be seen from the correlation matrix as shown in *Table 15*. A strong correlation among parameters of the first layer (0.8211), the second layer (–0.9327), and the third layer (0.9766) has been shown by the correlation matrix, which is comparable to the correlation matrix that has been presented by Sen et al. (1933 *Table 13*). A moderate correlation between fourth (–0.5246) and fifth layer parameters (0.4486) is also observed. It is also to be noticed that there is a sensible relation between sixth layer resistivity and fifth layer thickness, keeping the same model data.

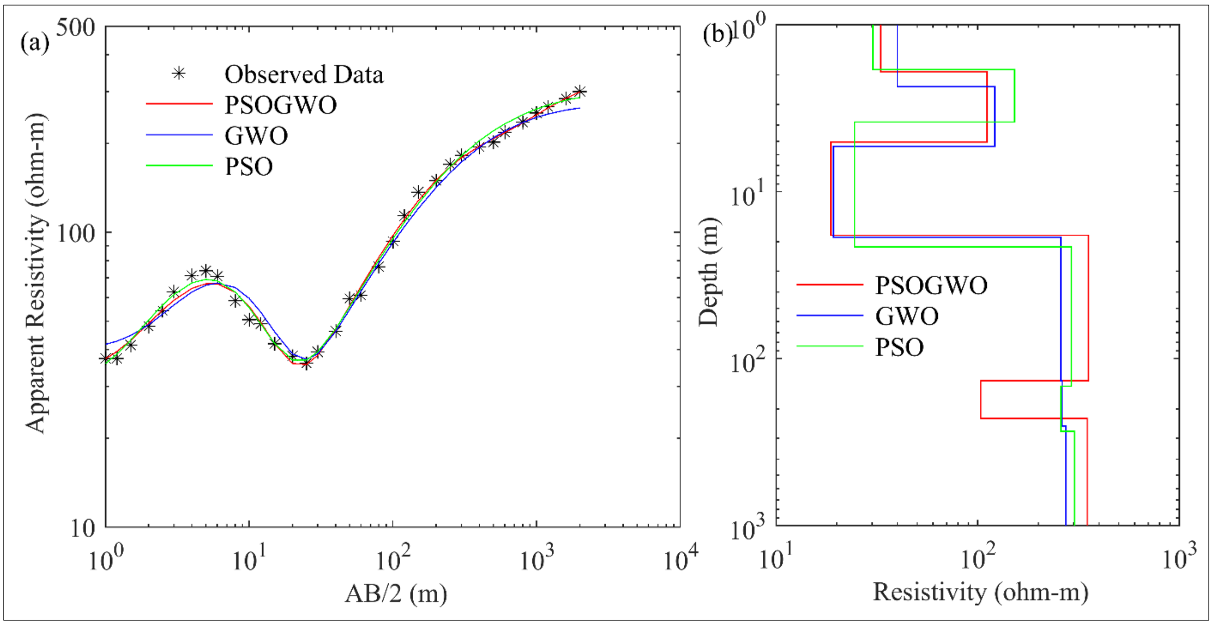

Figure 14. Six layer field data over Keshiari-Kharagpur near Kharagpur, India: (a) observed (*) and the best fitted calculated apparent resistivity curve (> 68.27% PDF); (b) one dimensional mean model (> 68.27% PDF) for true model (black colour), vPSOGWO (red colour), GWO (blue colour) and PSO (green colour).

The error differences in computed data with observed data are significant, as shown in *Fig. 14(a)* and *Table 12*. The inverted 1D layered models obtained from the mean model of 68.27% CI are shown in *Fig. 14(b)*. The computations time for vPSOGWO, GWO, and PSO are 3.58s, 3.44s, and 3.45s, respectively, for one run with 28 data points in this example. The inverted results from vPSOGWO, GWO, and PSO have been shown along with the borehole data, published result (Sen et al., 1993) in *Table 14*. It can note that the

-

outcomes from the hybrid algorithm satisfy the borehole information provided than the other algorithms and earlier published results.

Table 14. Optimization mean model result for six layer field resistivity sounding data.

Model Parameter	Search Range	Borehole Detail from Patella, 1975	Patella, 1975	Sen et al., 1993	Mean model (final 10000 sol.)			Mean model (PDF > 68.27%)		
					GWO	PSO	vPSOGWO	GWO	PSO	vPSOGWO
$\rho 1$ (Ωm)	10 - 50	- -	37	33 ± 4.91	36.47 ± 6.23	30.00 ± 8.49	32.93 ± 1.60	40 ± 2.41	30.24 ± 2.08	33.06 ± 0.57
$\rho 2$ (Ωm)	50 – 250	- -	140	240 ± 29.63	121.81 ± 29.04	158.49 ± 49.17	112.32 ± 24.59	121.42 ± 11.63	152.01 ± 20.51	111.25 ± 9.33
$\rho 3$ (Ωm)	1 – 40	- -	17	24 ± 1.37	19.38 ± 4.58	24.14 ± 7.07	18.19 ± 3.21	19.26 ± 1.85	24.49 ± 2.08	18.70 ± 1.15
$\rho 4$ (Ωm)	100 – 600	- -	340	300 ± 17.5	278.55 ± 71.41	299.07 ± 53.73	355.16 ± 42.70	258.02 ± 30.37	291.83 ± 23.55	354.49 ± 16.04
$\rho 5$ (Ωm)	30 - 500	- -	130	120 ± 32.09	276.27 ± 80.72	265.25 ± 65.06	105.80 ± 39.26	262.16 ± 33.24	259.27 ± 30.44	103.67 ± 14.50
$\rho 6$ (Ωm)	100 – 500	- -	300	320 ± 8.33	286.46 ± 46.72	303.76 ± 27.36	349.29 ± 20.98	273.73 ± 21.91	301.75 ± 12.34	349.68 ± 7.90
h1 (m)	0.5 – 3	1 (Aluvial soil)	1.3	1.1 ± 0.198	1.32 ± 0.48	0.96 ± 0.66	0.91 ± 0.09	1.36 ± 0.16	0.86 ± 0.10	0.92 ± 0.03
h2 (m)	1 – 8	3 (Fine sand)	2.7	1.3 ± 0.252	3.17 ± 0.98	2.13 ± 1.16	3.16 ± 0.47	3.01 ± 0.41	1.97 ± 0.34	3.13 ± 0.18
h3 (m)	1 – 25	12.5 (Calcarenite & sandy clay)	12	17 ± 1.13	13.66 ± 3.49	17.72 ± 6.03	12.93 ± 2.74	13.41 ± 1.36	17.57 ± 1.94	13.26 ± 1.02
h4 (m)	10 – 200	118.5 (Calcareous tufa & limestone)	120	125 ± 8.39	117.93 ± 33.89	124.38 ± 29.15	118.95 ± 30.44	117.28 ± 12.31	125.08 ± 13.71	117.72 ± 11.72
h5 (m)	10 – 200	65 (Water bearing limestone)	120	70 ± 23.15	118.79 ± 34.45	127.62 ± 29.37	93.12 ± 33.99	116.89 ± 12.36	125.98 ± 13.51	92.85 ± 13.03

Table 15. Correlation matrix using 68.27% PDF limit for six layer field resistivity sounding data.

-

Model Parmeter	ρ1 (Ωm)	ρ2 (Ωm)	ρ3 (Ωm)	ρ4 (Ωm)	ρ5 (Ωm)	ρ6 (Ωm)	h1 (m)	h2 (m)	h3 (m)	h4 (m)	h5 (m)
ρ1 (Ωm)	1.000	0.4779	–0.0875	–0.1111	0.0853	–0.0560	0.9324	–0.4458	–0.0868	0.0234	0.0152
ρ2 (Ωm)		1.000	0.3732	0.1178	–0.0770	0.1340	0.7174	–0.9018	0.3785	0.0674	0.0949
ρ3 (Ωm)			1.000	0.5415	–0.3876	0.3916	0.0045	–0.6603	0.9881	0.0207	0.1858
ρ4 (Ωm)				1.000	–0.6227	0.4864	–0.0878	–0.12579	0.6469	–0.4198	0.2740
ρ5 (Ωm)					1.000	–0.6675	0.0699	0.1727	–0.4580	–0.1085	0.0217
ρ6 (Ωm)						1.000	–0.0263	–0.2226	0.4484	0.3239	0.5275
h1 (m)							1.000	–0.6546	0.0059	0.0438	0.0327
h2 (m)								1.000	–0.6551	–0.0679	–0.1304
h3 (m)									1.000	–0.0324	0.2173
h4 (m)										1.000	–0.0142
h5 (m)											1.000

7.0 CONCLUSION

We have evaluated three meta-heuristic algorithms such as PSO, GWO, and vPSOGWO to realize their efficacy and applicability in the geoelectrical inverse problems, which narrates the appraisal of 1D resistivity models from geoelectrical resistivity sounding data. The relevance of these algorithms validated using synthetic and field resistivity sounding data signifying the kinds of earth's subsurface stratigraphy. An enormous solution 569 (100,000,000 from 10,000 runs) is assessed. Subsequently, the best-fitted solutions are chosen within a pre-distinct value for statistical measurements. The statistical study includes posterior PDF with 68.27% CI, a mean solution, posterior solution correlation matrix, and covariance matrix using search space, was carried out to refine the solutions to obtain the global mean solution with the least uncertainty. These statistical simulations yield essential information as to the reliability of an inversion algorithm. In general, conventional techniques can be quite effective in resolving the model in random noise but can fail in systematic error and inappropriate models. Our investigation with the

-

application of the developed algorithm, including statistical simulation for different multilayer resistivity parameters, resulted in a quantitative appraisal of uncertainty in the derived model parameters. We observed that the output of the hybrid algorithm in terms of mean model or error might be similar to either PSO or GWO (attributed to the exploration characteristics of GWO and exploitation characteristics of PSO). The vPSOGWO, GWO, and PSO algorithms performances have been analyzed based on the uncertainty and stability and mean model of layered earth structure. We found that the vPSOGWO gives very closer results than the results inverted from other two algorithms and also conventional methods which is consistently better than the previously published results, and correlated well with borehole information.

CONFLICT OF INTEREST

There are no conflicts of interest declared by the authors.

DATA AVAILABILITY STATEMENT

The support data of this study will be available on the request from corresponding authors. All the data taken for study to demonstrate our developed algorithms are a published/public domain data that obviously written in the manuscript.

REFERENCES

Colorni, A., Dorigo, M., Maniezzo, V., 1991. Distributed optimization by ant colonies. In Proceedings of the first European conference on artificial life 142, 134-142.

Dixon, O., Doherty, J. E., 1977. New interpretation methods for IP soundings. Exploration Geophysics 8, 65-69. https://doi.org/10.1071/EG977065.

Eiben, A. E., Schippers, C. A., 1998. On evolutionary exploration and exploitation. Fundamenta Informaticae 35, 35-50. https://doi.org/10.3233/FI-1998-35123403.

Esmin, A. A., Matwin, S., 2013. HPSOM: a hybrid particle swarm optimization algorithm with genetic mutation. International Journal of Innovative Computing, Information, and Control. 9, 1919-1934.

Kennedy, J., Eberhart, R., 1995. Particle swarm optimization. In Proceedings of ICNN'95-International Conference on Neural Networks IEEE 4, 1942-1948. https://doi.org/10.1109/ICNN.1995.488968.

Koefoed, O., 1979. Geosounding principles, 1: Resistivity sounding measurements. Methods in Geochemistry and Geophysics: Elsevier Science Ltd. Co., Amsterdam, 14A, pp 276.

Kamboj, V. K., 2015. A novel hybrid PSO–GWO approach for unit commitment Problem. Neural Computing and Applications 27(6), 1643-1655. https://doi.org/10.1007/s00521-015-1962-4.

Lai, X., Zhang, M., 2009. An efficient ensemble of GA and PSO for real function optimization. In 2009 2nd IEEE International Conference on Computer Science and Information Technology IEEE, 651-655. https://doi.org/10.1109/ICCIA.2010.6141614.

Mirjalili, S., Hashim, S. Z. M., 2010. A new hybrid PSOGSA algorithm for function optimization. In 2010 International conference on computer and information application IEEE, 374-377. https://doi.org/10.1109/ICCIA.2010.614161.

Mirjalili, S., Mirjalili, S.M., Lewis, A., 2014. Grey wolf optimizer. Advances in engineering software 69, 46-61. https://doi.org/10.1016/j.advengsoft.2013.12.007.

Mosegaard, K., Tarantola, A., 1995. Monte Carlo sampling of solutions to inverse problems. Journal of Geophysical Research Atmospheres 1001, 12431-12448. https://doi.org/10.1029/94JB03097.

-

Mitchell, M., 1998. An introduction to genetic algorithms. A Bradford Book, The MIT Press.

Narayan, S., Dusseault, M. B., Nobes, D. C., 1994. Inversion techniques applied to resistivity inverse problems. Inverse Problems 10, 669–686.

Oldenburg, D. W., Li, Y., 1994. Inversion of induced polarization data. Geophysics 59, 1327–1341. https://doi.org/10.1190/1.1443692.

Panda, K. P., Sharma, S. P., Jha, M. K., 2018. Mapping lithological variations in a river basin of West Bengal, India using electrical resistivity survey implications for artificial recharge. Environmental Earth Sciences 77, 1-10. https://doi.org/10.1007/s12665-018-7813-8.

Parasnis D. S., 1980. Principles of Applied Geophysics. Fourth ed., New York, Chapman, and Hall.

Pekeris, C. L., 1940. Direct method of interpretation in resistivity prospecting. Geophysics 5, 31-42. https://doi.org/10.1190/1.1441791.

Rashedi, E., Nezamabadi-Pour, H., Saryazdi, S., 2009. GSA: a gravitational search algorithm. Information sciences 179, 2232-2248. https://doi.org/10.1016/j.ins.2009.03.004.

Roshan, R., Singh, U. K., 2017. Inversion of residual gravity anomalies using tuned PSO. Geoscientific Instrumentation Methods and Data Systems 6, 71-79. https://doi.org/10.5194/gi-6-71-2017.

Ross, S., 2009. Probability and statistics for engineers and scientists. Elsevier, New Delhi, 16, 32-33.

Sen, M. K., Bhattacharya, B. B., Stoffa, P. L., 1993. Nonlinear inversion of resistivity sounding data. Geophysics 58, 496-507. https://doi.org/10.1190/1.1443432.

-

Şenel, F. A., Gökçe, F., Yüksel, A. S., Yiğit, T., 2019. A novel hybrid PSO–GWO algorithm for optimization problems. Engineering with Computers 35, 1359-1373. https://doi.org/10.1007/s00366-018-0668-5.

Singh, N., Singh, S. B., 2017. Hybrid algorithm of particle swarm optimization and grey wolf optimizer for improving convergence performance. Journal of Applied Mathematics, 1-15. https://doi.org/10.1155/2017/2030489.

Singh, U. K., Tiwari, R.K., Singh, S.B., 2005. One-dimensional inversion of geo-electrical resistivity sounding data using artificial neural networks—a case study. Computers & Geosciences 31, 99-108. https://doi.org/10.1016/j.cageo.2004.09.014.

Singh, U. K., Tiwari, R.K., Singh, S.B., 2013. Neural network modeling and prediction of resistivity structures using VES Schlumberger data over a geothermal area. Computers & Geosciences 52, 246-257. https://doi.org/10.1016/j.cageo.2012.09.018.

Sharma, S. P., 2012. VFSARES—a very fast simulated annealing FORTRAN program for interpretation of 1-D DC resistivity sounding data from various electrode arrays. Computers & Geosciences 42, 177-188. https://doi.org/10.1016/j.cageo.2011.08.029.

Simon, D., 2008. Biogeography-based optimization: IEEE transactions on evolutionary computation 12, 702-713. https://doi.org/10.1109/TEVC.2008.919004.

Storn, R., Price, K., 1997. Differential evolution–a simple and efficient heuristic for global optimization over continuous spaces. Journal of global optimization 11, 341-359. https://doi.org/10.1023/A:1008202821328.

Whitley, D., 1994. A genetic algorithm tutorial, Statistics and Computing 4, 65-85. https://doi.org/10.1007/BF00175354.

-

Yang, X.S., 2010. A new metaheuristic bat-inspired algorithm. In nature inspired cooperative strategies for optimization (NICSO 2010), Springer, Berlin, Heidelberg. 65-74. https://doi.org/10.1007/978-3-642-12538-6_6.